

Rectification in a Stochastically Driven Three-Junction SQUID Rocking Ratchet

A. Sterck, D. Koelle, and R. Kleiner*

*Physikalisches Institut and Center for Collective Quantum Phenomena, Universität Tübingen,
Auf der Morgenstelle 14, D-72076 Tübingen, Germany*

(Received 6 May 2009; published 22 July 2009)

A three-junction SQUID forms a rocking ratchet for the phase differences across the Josephson junctions. In this Letter we investigate its capability to rectify voltages under stochastic drive currents with a white frequency spectrum up to a cutoff frequency f_{cut} . Experimentally, we accessed the adiabatic regime and find very good agreement with theory. Numerically, we also investigated large values of f_{cut} and find, in agreement with the laws of thermodynamics, that the response disappears, as f_{cut} becomes much larger than the characteristic frequency scales of the system.

DOI: 10.1103/PhysRevLett.103.047001

PACS numbers: 85.25.Dq, 05.40.-a, 05.60.-k, 74.40.+k

Originally motivated by the discovery of molecular motors in biological systems [1,2], the investigation of ratchets became an intense field of research [3,4]. In the simplest case, a ratchet consists of a particle moving (on average) directionally in an asymmetric periodic potential under the action of random or periodic forces with zero time average. Particularly the directional motion in the presence of random forces is somewhat counterintuitive, resulting in a perpetuum mobile of the second kind if the system were in thermal equilibrium [5]. However, the ratchet effect is not forbidden by thermodynamics if the fluctuations are far from equilibrium [3,4].

In superconductivity, ratchets have been studied on the basis of moving Abrikosov [6–10] or Josephson [11–15] vortices, or by monitoring the phase difference of the superconducting wave function across Josephson junctions in specially designed superconducting quantum interference devices (SQUIDs) [16–20]. In the latter case the energy stored in the junctions together with the magnetic energy in the SQUID loop creates a ratchet potential for a fictitious particle the velocity of which is monitored via the voltage drop across the junctions. A bias current (with vanishing time average) tilts the potential and thus realizes a rocking ratchet.

To our knowledge all experimental investigations performed so far on these ratchets focused on either purely deterministic drive forces or considered modifications of the deterministic response upon addition of brown noise [13]. For other ratchet systems, rectifying fluctuations were, e.g., studied experimentally in optical lattices [21,22], in biological systems [23], or in electronic analog circuits [24]. However, in general, experimental investigations for the case of pure stochastic drives are rare.

In this Letter we study the ratchet effect under purely stochastic drives for a SQUID ratchet containing 3 Josephson junctions. This type of ratchet has been characterized in terms of periodic drives in Ref. [20] and was based on a theoretical proposal by Zapata *et al.* [16] with some modifications. The device is schematically shown in Fig. 1(a). The SQUID is biased by a current I and a

magnetic flux Φ_a is applied to the loop. The Josephson phase differences δ_k , with $k = 1, 2, 3$, act as three generalized coordinates. One obtains a periodic potential U which is asymmetric for a proper choice of the maximum supercurrents I_{0k} of the three junctions. U can be expressed as a function of δ_3 and $\delta_l = \delta_1 + \delta_2$, [20]. In the limit $\beta_L \equiv 2I_0L/\Phi_0 \ll 1$, where L is the inductance of the ring, Φ_0 is the flux quantum and $I_0 = (I_{01} + I_{03})/2$, U becomes a function of δ_l only. Its shape can be controlled by Φ_a ; see Fig. 2 in Ref. [20]. For $I_{01} \approx I_{02}$, as in our experiment, $U(\delta_l) = I_{01}[s \cos(\delta_l + 2\pi\Phi_a/\Phi_0) + 2 \cos(\delta_l/2)]$, where $s = I_{03}/I_{01}$. Using Kirchhoff's laws, Josephson's equations and the resistively and capacitively shunted junction model [25,26] one obtains a system of three coupled Langevin equations for the δ_k [20]. In the mechanical picture, the current I represents the force that pushes the particle in the direction δ_l and the voltage $\tilde{U} = (\Phi_0/2\pi)\dot{\delta}_l$ across the SQUID measures the (instant) velocity in this direction. The dc voltage across the SQUID [denoted V for current voltage characteristics (IVCs) and V_{dc} for the ratchet response] is obtained by time averaging \tilde{U} . The Langevin equations introduce as additional parameters the

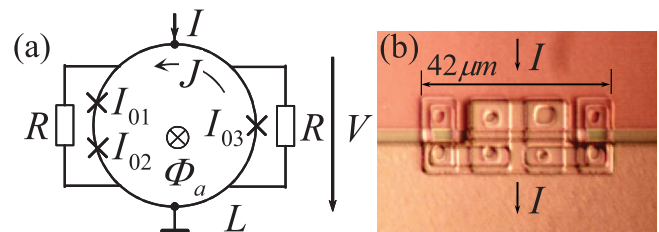


FIG. 1 (color online). Schematic (a) and optical image (b) of the three-junction SQUID consisting of a superconducting ring of inductance L interrupted by two Josephson junctions in its left arm and one in its right arm. The SQUID is fed by a current I , an applied flux Φ_a tunes the operation point. The crosses symbolize the junctions; their maximum supercurrents are denoted I_{0k} , with $k = 1, 2, 3$. Junctions 1 and 2 are shunted by a common resistor R ; junction 3 is shunted separately by a resistor which, by design, has the same magnitude R . J denotes the screening current around the ring.

product $I_0 R$, where R is the shunt resistance; cf. Fig. 1(a). $I_0 R$ and the characteristic frequency $f_c = I_0 R / \Phi_0$ act as scaling parameters. An important quantity is the noise parameter $\Gamma = 2\pi k_B T / I_0 \Phi_0$ associated with Nyquist noise arising from the shunt resistors [27]. Note that, due to normalization to the bandwidth f_c , Γ does not contain R explicitly. The factor $2\pi k_B T / \Phi_0$ can be seen as the mean amplitude of the fluctuation current ($0.18 \mu\text{A}$ at 4.2 K). One further has the capacitance parameters $\beta_{ck} = 2\pi C_k I_0 R^2 / \Phi_0$, with $k = 1, 2, 3$. In our experimental situation, β_{ck} and β_L are very small (of order 10^{-2}) and affect calculated properties only marginally. Thus, the relevant device parameters are $I_0 R$, Γ , and s .

Figure 1(b) shows an optical image of the three-junction SQUID. It was fabricated at HYPRES [28] using standard Nb/Al-AIO_x/Nb technology with junctions of nominal critical current density $j_0 = 100 \text{ A/cm}^2$ at $T = 4.2 \text{ K}$ and a capacitance per area of $C' = 38 \text{ fF}/\mu\text{m}^2$. In Fig. 1(b) parts of the contacting electrodes, formed by the upper of two Nb layers, appear as the two homogeneous areas in the upper and lower halves of the image. They are separated by a gap bridged by the Josephson junctions and the shunt resistors. The shunts (outer rectangles) consisting of a Au/Pd layer are connected to the electrodes by circular vias. The second rectangle from the left (located in the lower Nb layer) contains junctions 1 and 2 of areas $A_{J,1} = A_{J,2} \approx 11.3 \mu\text{m}^2$ that are visible as circular structures inside the rectangle. Junction 3 (area $A_{J,3} \approx 5.3 \mu\text{m}^2$) is embedded in the second rectangle from the right which also contains a via to the upper Nb layer. All transport measurements were performed at $T = 4.2 \text{ K}$ in a magnetically and electrically shielded environment. Signals were transferred to the SQUID via the leads contacting the SQUID. To guarantee a broadband signal transfer no additional (low pass) filters were mounted in the current leads, at the expense of an enhanced pickup of environmental noise. To obtain IVCs the device was biased with a static current I . To investigate the ratchet effect the device was either, for reference, biased with a monochromatic drive of frequency f (here we discuss the case $f = 50 \text{ kHz}$) or with a stochastic drive, implemented by an Agilent 33250A arbitrary wave form generator producing Gaussian voltage noise with a bandwidth of 50 MHz . In the stochastic case a variable resistor R_v operated in the $10 \text{ k}\Omega$ range was mounted in series with the SQUID to control the amplitude of the drive current. R_v is much higher than the SQUID impedance including the leads; thus the current through the SQUID to a good approximation has a white spectral power distribution up to the cutoff frequency $f_{\text{cut}} = 50 \text{ MHz}$. Note that both the deterministic and the stochastic drive are essentially adiabatic (for a discussion of non-adiabatic monochromatic drive frequencies, see Ref. [20]). As we will see, f_c is about 7.7 GHz and thus much higher than f or f_{cut} . The same holds for other characteristic time scales of the device (such as the LC resonance frequency of the loop) which are well above f_c .

Let us first characterize the device in terms of dc properties, device parameters, and the ratchet effect for the monochromatic drive. To find the relevant junction and SQUID parameters, having design values as a starting point, we compare numerical simulations and measurements of the IVC at zero applied flux, plus the dependence of the maximum supercurrent of the device on applied flux (I_c vs Φ_a). Figure 2(a) shows the measured IVC at $\Phi_a = 0$ (open circles) together with a simulated curve (solid line). For the simulation the Langevin equations have been integrated over $10^3 \pi$ time units per point, with a lower cutoff of 0.2 (the time unit is given by $1/2\pi f_c$). Fitting of the simulated IVC to the measured curve yields $2I_0 = 29.9 \mu\text{A}$ and $I_0 R = 16 \mu\text{V}$ and thus $f_c \approx 7.7 \text{ GHz}$. The critical current density j_0 is about 180 A/cm^2 and thus somewhat higher than expected. By contrast, $R \approx 1.07 \Omega$ is close to the design value. Note that the IVC is substantially rounded near I_c , requiring a noise parameter $\Gamma = 0.09$ which, most likely due to environmental noise (kHz to tens of GHz due to radio and mobile stations, computers, etc.), is about 7.6 times higher than estimated from I_0 and the bath temperature of 4.2 K . We further used $s = 0.4$, which is somewhat smaller than the design value of 0.5 . While the IVC at $\Phi_a = 0$ is not very sensitive to s , the dependence $I_c(\Phi_a)$ is, and Fig. 2(b) shows the corresponding measurement (open circles) and simulation (line). Note that, due to the substantial noise rounding of the IVC the “critical current” needs to be defined and measured using a voltage criterion for which we have used $1 \mu\text{V}$ in the experiment and $0.07 \text{ V}/I_0 R$ in the simulations. From the values of s and I_0 we obtain $I_{03} \approx 8.5 \mu\text{A}$ and $I_{01} \approx 21.5 \mu\text{A}$. We further assumed that $I_{02} = 1.01 I_{01}$. (For $I_{01} = I_{02}$ unrealistic solutions appear; e.g., the IVC at $\Phi_a/\Phi_0 = 0.25$ has a 30% higher I_c . This effect disappears when I_{01} differs from I_{02} by 10^{-5} or even less and thus seems impossible to observe.) Further, from geometry we estimate $L \approx 1.1 \text{ pH}$ and thus $\beta_L \approx 0.016$. For β_{ck} we estimate values of about 0.04 for junctions 1 and 2 and 0.008 for junction 3. For the simulations we have used somewhat larger values, $\beta_L = 0.1$ and $\beta_{ck} = 0.15 I_k / I_0$. This only marginally affects the calculated SQUID characteristics (in turn not allowing a determination of L and the C_k with accuracy beyond the design values) but greatly improves computation times, becoming very large for $\beta_L, \beta_{ck} \rightarrow 0$. Having fixed all model parameters now for the curves discussed below there are no more free parameters.

To further characterize our device we have measured at $\Phi_a = 0.25 \Phi_0$ its response V_{dc} upon a 50 kHz (corresponding to $f/f_c \approx 6.5 \times 10^{-6}$) monochromatic drive, $I_{ac} \cos 2\pi f t$. The result is shown by open symbols in Fig. 2(c). To compare this curve with theory we first note that in the adiabatic case the basic information about the ratchet is contained in the IVC. For $f/f_c \rightarrow 0$ we thus can find V_{dc} by integrating $V(I)$ over a distribution of I values representing the ac drive. We thus first determine by a full numeric simulation the IVC at $\Phi_a = 0.25 \Phi_0$, using an

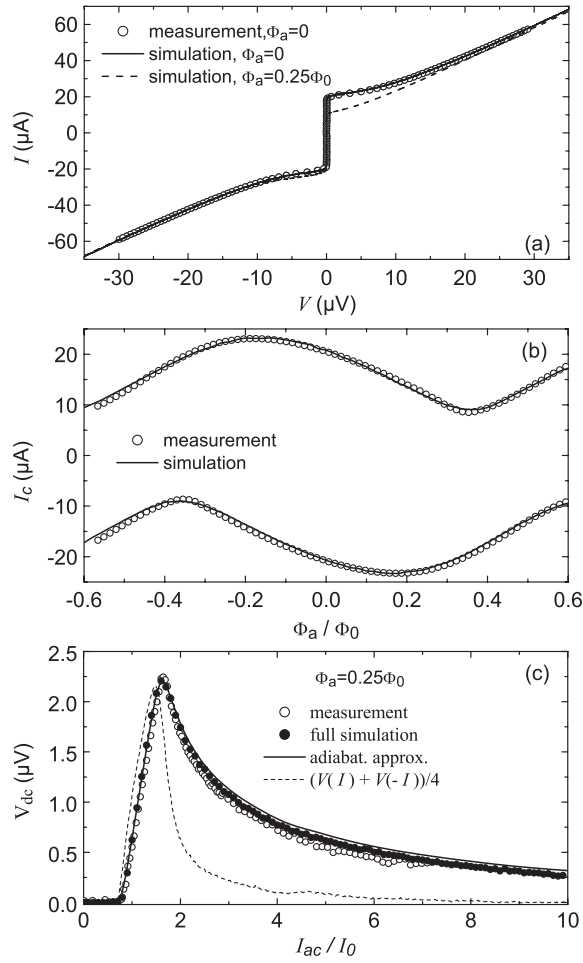


FIG. 2. Characterization of the three-junction SQUID ratchet. (a) Measured IVC at $\Phi_a = 0$ (open circles) together with the simulated curve (solid line). Dashed line: calculated IVC for $\Phi_a = 0.25\Phi_0$. (b) I_c vs Φ_a . Open symbols: measurement; solid line: simulated curve. Relevant model parameters: $2I_0 = 29.9 \mu\text{A}$, $I_0R = 16 \mu\text{V}$ ($f_c \approx 7.7 \text{ GHz}$), $s = 0.4$, and $\Gamma = 0.09$. (c) V_{dc} vs I_{ac} for a $f = 50 \text{ kHz}$ monochromatic drive (open symbols, $f/f_c = 6.5 \times 10^{-6}$) together with simulated curves. Solid markers: full numerical simulation, with $f/f_c = 0.005$; solid line: approximate solution using the calculated IVC at $\Phi_a = 0.25\Phi_0$. For comparison, the dashed line shows the asymmetry in dc voltages $[V(+I) + V(-I)]$, as determined from the calculated IVC. This curve, plotted using the ordinate for I and the abscissa for V , has been divided by 4 to become comparable in magnitude to the other curves.

integration time of $3 \times 10^4 \pi$ and then use this curve to calculate the ratchet response via $V_{dc} = \int_{-I_{ac}}^{I_{ac}} V(I)p(I)dI$. For a monochromatic drive with amplitude I_{ac} the distribution function p is given by $1/[\pi(I_{ac}^2 - I^2)^{0.5}]$. The calculated ratchet response agrees reasonably well with the data, although V_{dc} is somewhat overestimated at large values of I_{ac} . For comparison, we show by black circles also a curve where we have fully integrated the Langevin equations using $f/f_c = 0.005$ (the much lower experimental value would require enormous computing times). The corresponding curve lies within the measured data and the

approximated curve. The small but clearly visible deviation from the latter curve at large values of I_{ac} is actually caused by the increasingly growing sweep rate dI/dt in the vicinity of maximum asymmetry. We confirmed this by solving the Langevin equations for $I_{ac}/I_0 = 10$ for $f/f_c = 10^{-3}$; the difference to the adiabatic curve decreased by 50% in this case. The difference of the experimental curve to the theoretical ones may be caused by a similar effect.

As the main result, Fig. 3 shows the response of our device upon a stochastic drive with standard deviation I_{noise} and $f_{cut} = 50 \text{ MHz}$, corresponding to $f_{cut}/f_c = 0.0065$. Figure 3(a) displays by open circles V_{dc} vs Φ_a for a fixed value $I_{noise} = 1.1I_0$. V_{dc} varies periodically with Φ_a , reaching a maximum value of $0.077 I_0R$ ($1.23 \mu\text{V}$) at $\Phi_a = 0.33\Phi_0$. This maximum response is only about a factor of 1.8 smaller than for the deterministic case discussed above. The simulated curve (fully solving the Langevin equations), shown by closed circles, agrees very well with the measurement. The same holds for the case shown in Fig. 3(b) where we have investigated V_{dc} vs I_{noise} at $\Phi_a = 0.25\Phi_0$. Measured data are shown by open circles. Here, the maximum rectified voltage of $0.077I_0R$ is reached at $I_{noise} = 1.54I_0$. Further note that, since in the stochastic case even at low values of I_{noise} there is a finite probability for a large amplitude current fluctuation, the onset of the nonzero V_{dc} is much lower and less sharp than

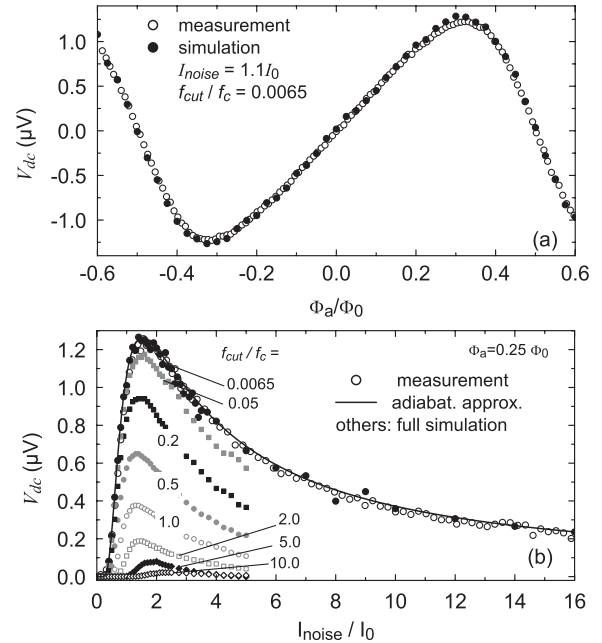


FIG. 3. The response V_{dc} of the three-junction SQUID ratchet to stochastic drives. (a) V_{dc} vs Φ_a at fixed $I_{noise} = 1.1I_0$. (b) V_{dc} vs I_{noise}/I_0 at $\Phi_a = 0.25\Phi_0$. Open black circles in both graphs: measured data, obtained with $f_{cut} = 50 \text{ MHz}$. Solid black circles in both graphs: full numerical simulation, with $f_{cut} = 0.0065f_c$ (corresponding to the experimental value). Solid line in (b) approximated theoretical curve valid for $f_{cut}/f_0 \rightarrow 0$. Other curves in (b) series of full numeric simulations for 7 larger values of f_{cut}/f_0 between 0.05 and 10.

for the periodic drive. The simulated curve is shown by black circles. The adiabatic drive was created by a sequence of Gaussian distributed random numbers, cutting its spectrum at $f_{\text{cut}}/f_c = 0.0065$ and, after backtransformation to the time domain, normalizing it to $I(t) = I_{\text{noise}}g(t)$, where $g(t)$ has a standard deviation of 1. The integration time required to achieve a given accuracy in V_{dc} increases $\propto I_{\text{noise}}^2$. Thus, for $I_{\text{noise}}/I_0 < 1.1$ the voltage across the SQUID was integrated over $\tau = 5 \times 10^6 \pi$ time units, with a time step of $\Delta\tau = 0.2$ time units. For $1.1 < I_{\text{noise}}/I_0 < 3.5$, $\tau = 2 \times 10^7 \pi$ was used, which was further increased to $\tau = 10^8 \pi$ for $3.5 < I_{\text{noise}}/I_0 < 10$ and to $\tau = 10^9 \pi$ for larger values of I_{noise} . The simulated curve agrees excellently with the measured data. The same holds for the approximated curve, where, similar to the case of the monochromatic drive, the IVC at $\Phi_a = 0.25\Phi_0$ was integrated, using the distribution function $p(I) = \exp(-I^2/2I_{\text{noise}}^2)/(\sqrt{2\pi}I_{\text{noise}})$. The integral should be evaluated from $-\infty$ to ∞ . However, the asymmetry $V(+I) + V(-I)$ in the IVC becomes very small for large values of I/I_0 ; cf. dashed line in Fig. 2(c). We thus have limited the integration to $\pm 10I_0$. Further note that the environmental noise may add to the applied noise current. From the value $\Gamma = 0.09$ obtained from analyzing the IVC we obtain a corresponding rms noise current of about $1.4 \mu\text{A}$. Assuming (worst case) that this noise fully appears at frequencies below f_{cut} one expects V_{dc} vs I_{noise}/I_0 to be shifted by 0.09. However, this effect is smaller than the symbol size in Fig. 3 and thus negligible.

Having very good agreement between theory and experiment for the adiabatic case one can ask in which way the ratchet response disappears when f_{cut} is increased, finally leading to a white spectral power distribution of current values. Figure 3(b) shows 7 simulated curves where f_{cut}/f_c was increased from 0.05 to 10 (we are not equipped to study these cutoff frequencies experimentally). As can be seen the ratchet response gradually decreases with increasing f_{cut}/f_c and is barely visible for $f_{\text{cut}}/f_c = 10$. Note that, if, instead of a function generator, the stochastic current (with its spectrum cut off by some capacitor) would have been produced by a hot resistor R_h at temperature T_R , the low frequency noise current would be given by $I_{\text{noise}} = (4k_B T_R f_{\text{cut}}/R_h)^{1/2}$. Assuming for simplicity $R_h = 10 \Omega$ ($\approx 10R$), in order to justify its description as a current source, one obtains $I_{\text{noise}}/I_0 = 1$ at $T_R \approx 8 \times 10^5 \text{ K}$ for $f_{\text{cut}} = 50 \text{ MHz}$. Even if the bandwidth is increased to $f_{\text{cut}}/f_c = 10$, where the ratchet response has almost disappeared, the temperature of the resistor would still be as high as 500 K. Thus, for all cases, the SQUID ratchet clearly needs to be driven in a nonequilibrium situation.

In summary, the SQUID ratchet studied in this work exhibits a relatively large voltage response upon an adiabatic stochastic drive current, which is white up to a cutoff frequency $f_{\text{cut}} = 50 \text{ MHz}$. The response can be well re-

produced both by direct simulations using the Langevin equations for the SQUID dynamics and by a semianalytic approach, based on integrating the current voltage characteristic of the device with a Gaussian distribution of drive current values. Numerically, we also investigated the case of large values of f_{cut} and find, in agreement with the laws of thermodynamics, that the ratchet response gradually disappears when f_{cut} becomes larger than the characteristic frequency scales of the device.

We thank P. Reimann and E. Goldobin for valuable discussions. Financial support from the Deutsche Forschungsgemeinschaft via project KO1303/7 is gratefully acknowledged.

*kleiner@uni-tuebingen.de

- [1] F. Jülicher, A. Adjari, and J. Prost, *Rev. Mod. Phys.* **69**, 1269 (1997).
- [2] R.D. Astumian, *Science* **276**, 917 (1997).
- [3] P. Reimann, *Phys. Rep.* **361**, 57 (2002).
- [4] P. Hänggi and F. Marchesoni, *Rev. Mod. Phys.* **81**, 387 (2009).
- [5] R.P. Feynman, R.B. Leighton, and M. Sands, *The Feynman Lectures on Physics* (Addison-Wesley, Reading, MA, 1966), Vol. I, Chap. 46.
- [6] J.F. Wambaugh *et al.*, *Phys. Rev. Lett.* **83**, 5106 (1999).
- [7] C.-S. Lee *et al.*, *Nature (London)* **400**, 337 (1999).
- [8] C.J. Olson *et al.*, *Phys. Rev. Lett.* **87**, 177002 (2001).
- [9] J.E. Villegas *et al.*, *Science* **302**, 1188 (2003).
- [10] J. Van de Vondel *et al.*, *Phys. Rev. Lett.* **94**, 057003 (2005).
- [11] E. Trías *et al.*, *Phys. Rev. E* **61**, 2257 (2000).
- [12] E. Goldobin, A. Sterck, and D. Koelle, *Phys. Rev. E* **63**, 031111 (2001).
- [13] G. Carapella and G. Costabile, *Phys. Rev. Lett.* **87**, 077002 (2001).
- [14] G. Carapella, *Phys. Rev. B* **63**, 054515 (2001).
- [15] M. Beck *et al.*, *Phys. Rev. Lett.* **95**, 090603 (2005).
- [16] I. Zapata *et al.*, *Phys. Rev. Lett.* **77**, 2292 (1996).
- [17] S. Weiss *et al.*, *Europhys. Lett.* **51**, 499 (2000).
- [18] A. Sterck, S. Weiss, and D. Koelle, *Appl. Phys. A* **75**, 253 (2002).
- [19] J. Berger, *Phys. Rev. B* **70**, 024524 (2004).
- [20] A. Sterck, R. Kleiner, and D. Koelle, *Phys. Rev. Lett.* **95**, 177006 (2005).
- [21] P.H. Jones, M. Goonasekera, and F. Renzoni, *Phys. Rev. Lett.* **93**, 073904 (2004).
- [22] C. Mennerat-Robilliard *et al.*, *Phys. Rev. Lett.* **82**, 851 (1999).
- [23] T.D. Xie *et al.*, *Biophys. J.* **72**, 2496 (1997).
- [24] A.P. Nikitin and D.E. Postnov, *Tech. Phys. Lett.* **24**, 61 (1998).
- [25] W.C. Stewart, *Appl. Phys. Lett.* **12**, 277 (1968).
- [26] D. McCumber, *J. Appl. Phys.* **39**, 3113 (1968).
- [27] C.D. Tesche and J. Clarke, *J. Low Temp. Phys.* **29**, 301 (1977).
- [28] HYPRES, Elmsford, NY, <http://www.hypres.com>